Assessment of water and food security nexus under climate change using a seamless modelling framework

Mohamed Rasmy[1], Koki Homma[2], Miho Ohara[1], Tomoki Ushiyama[1], Ralph Acierto[1], and Toshio Koike[1]
International Centre for Water Hazard and Risk Management (ICHARM), Public Work Research Institute, Japan[1]
E-mail: abdul@pwri.go.jp
Graduate School of Agricultural Science, Tohoku University, Japan [2]
E-mail: koki.homma.d6@tohoku.ac.jp

ABSTRACT

Climate change has led to an increase in hydro-meteorological extremes, which have significant and often devastating impacts on lives, economies and agricultural production. It is crucial to quantify the impact of climate change on water availability, hydro-climatic extremes and agricultural productivity for sustainable basin-scale planning. Previous studies have not fully investigated the impact on the water-food nexus using an integrated approach. To address this, the research project has developed a seamless modelling framework that integrates the latest scientific and technological advances, such as Global Climate Model (GCM) outputs and downscaling techniques, as well as seamless hydrological and crop modelling. This research therefore presents a reliable method of quantifying the impact of climate change on water and food security, taking advantage of the latest scientific and technological advances. These include GCM outputs for past (1979–2003) and future (2075–2099) climates under two scenarios (RCP2.6 and RCP8.5); downscaling techniques; and a seamless Water and Energy Budget-based Rainfall-Runoff-Inundation (WEB-RRI) model coupled with a Simulation Model for Rice–Weather Relations (SIMRIW) model. The results indicated an increase in annual and seasonal rainfall under both RCP2.6 and RCP8.5 scenarios, particularly during the wet season, with enhanced intra-basin variability. The basin's hydrological response showed increased river discharge, with the future scenarios indicating higher mean flows, greater seasonal peaks, and an amplification of extreme high-flow events. Projections of rice yield reveal that the future climate under RCP2.6 will produce relatively minor yield reductions, whereas RCP8.5 will lead to widespread yield declines due to the combined effects of rising temperatures, altered rainfall patterns and increased hydrological extremes. The results of this study show that hydro-climatic extremes will increase significantly under higher emission pathways (RCP8.5). This threatens food security and highlights the importance of climate-informed strategies for managing water and agriculture in the basin, in order to enhance resilience and sustainability.

KEYWORDS: Climate change, hydrological modelling, crop modelling, crop yield change

1 INTRODUCTION

Climate change threatens water security by disrupting the water cycle and accelerating extreme weather events such as floods and droughts. Water is also central to agriculture, a key driver of sustainable socio-economic growth, livelihoods and food security. Food production depends heavily on water availability, as irrigation accounts for a significant proportion of global water withdrawals, and is often affected by hydro-meteorological extremes. As climate change continues to exacerbate water and food insecurity (IPCC, 2022), it is crucial to develop disaster risk reduction (DRR) policies in a changing climate to ensure sustainable development. The development of DRR policies relies on the reliable quantification of the impact of climate change on water availability, water-related disasters and agricultural production. Previous studies have used simulation models to quantify the impact of climate change on water-related disasters and crop damage separately. However, no studies have investigated the combined effects of floods, droughts and water availability on crop yield under changing climatic conditions simultaneously. Consequently, this research proposes a method to reliably quantify the impact of climate change on water and food security, leveraging the latest scientific and technological advancements such as Global Climate Model (GCM) outputs, downscaling techniques, and integrated hydrological and crop modelling.

GCMs are fundamental tools for projecting future climate changes; however, their outputs cannot be utilised directly in basin-scale hydro-crop models due to model-related uncertainties, coarse resolutions and unrealistic representations of basin-scale precipitation information (Zhang et al., 2016). Studies have shown that high-resolution GCMs (i.e. with a resolution of ~20–60 km or less) improve rainfall simulation (Kusunoki, 2015). However, the outputs of these models are still too coarse for climate change impact assessment studies on water availability and food production at relatively small and medium-sized basins. To address these resolution issues, regional climate models (RCMs) can be employed to enhance atmospheric variables, including extreme rainfall events (Rockel, 2015). To further improve bias originating from the parent GCM and parameterisation processes, statistical bias correction methods are employed, involving the derivation of statistical transfer functions from long-term ground data and past GCM outputs (Moghim et al., 2017). Therefore, using bias-corrected, high-resolution RCM rainfall outputs for climate change impact studies is preferable given their superior performance in simulating rainfall amounts and distributions.

Moreover, distributed hydrological models (DHMs) are essential tools for simulating various hydrological processes under past and future climatic conditions. They provide policymakers with evidence-based information on water resources and water-related disasters (Sayama et al., 2010; Zheng et al., 2021). As floods and droughts are likely to intensify and often occur in succession in a warming climate, it is necessary to manage these two extremes in an integrated way rather than addressing them as separate hazards. In order to seamlessly simulate floods and droughts as well as assess their impact on crop production, the hydrological model must be physically based and capable of addressing parameters related to floods (e.g. peak flood discharge and inundation), droughts (e.g. soil moisture, evapotranspiration (ET) and low flow discharges) and crop growth (e.g. soil moisture and temperature) simultaneously. Rasmy et al. (2019) developed the Water and Energy Budget-Based Rainfall-Runoff-Inundation (WEB-RRI) model, which considers water- and energy-related processes, as well as soil moisture dynamics, ET and runoff and inundation processes. It is an appropriate model for reliably simulating basin hydrological responses under water cycle variability and climate change.

Furthermore, paddy rice is a staple food globally and its cultivation occupies a significant portion of food production systems worldwide. In this study, we adopted the SIMRIW-Rain-fed model (Homma and Horie, 2009), a simplified, process-based model for simulating the growth and yield of irrigated rice. The model simulates three major processes: plant ontogenetic development; leaf area expansion; and dry matter accumulation. It has been validated in many regions, including Japan, the USA, Thailand, Indonesia and Lao PDR (Homma and Horie, 2009; Homma et al., 2017; Maki et al., 2017; Raksapatcharawong et al., 2020).

Consequently, this paper assessed the impact of climate change on hydro-meteorological characteristics and their effect on paddy yields, using high-resolution climate model outputs from MRI-AGCM-3.2H (with a resolution of ~60 km) for two extreme Representative Concentration Pathway (RCP) scenarios (i.e. RCP2.6 and RCP8.5). This was achieved through RCM downscaling of MRI-AGCM-3.2H data, as well as using the WEB-RRI and SIMRIW models in the Pampanga River basin in the Philippines.

2 METHOD, STUDY AREA, DATA, AND MODEL SET-UP

2.1 Method

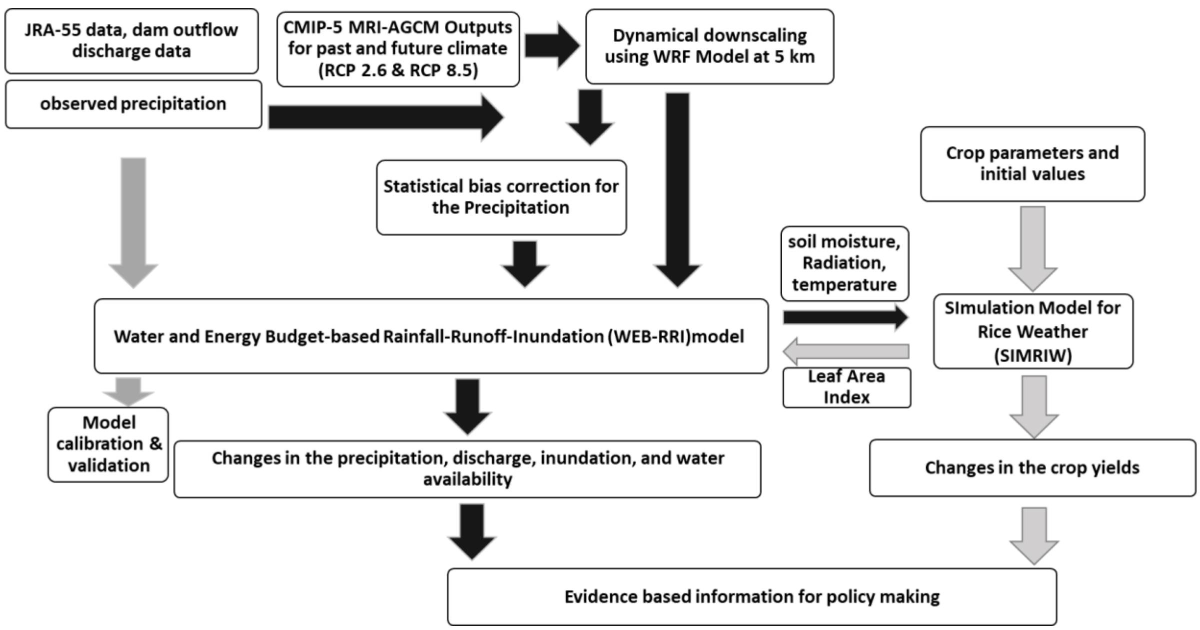

Figure 1. The research framework of climate change impact assessment on the water resources and paddy rice production

This research presents a method of assessing the impact of climate change on water and food security (Fig. 1). The proposed method involves dynamical downscaling of the MRI-AGCM from a horizontal resolution of 60 km to 5 km, and the statistical bias correction of the resulting rainfall data using long-term daily rainfall observations from several gauging stations. A hybrid WEB-RRI-SIMRIW model was developed, calibrated and validated using in situ data. This model was then used to evaluate changes in water resources, water-related disasters and paddy yield in future climates. The following subsections briefly describe the major components and procedures shown in Fig. 2.

2.2 Study area and Data

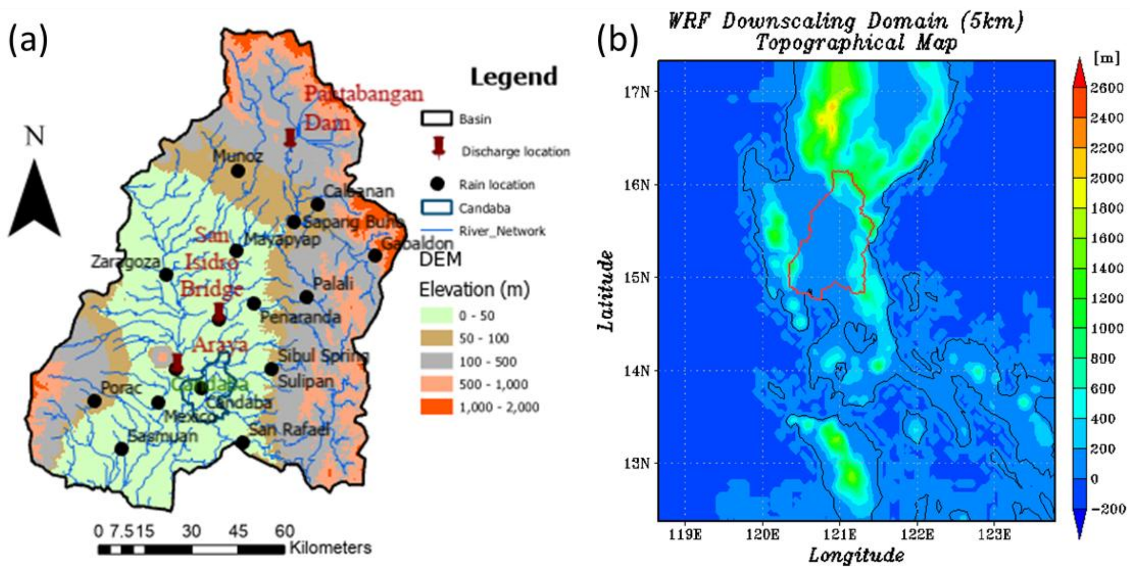

Figure 2: Study area, gauge locations, and simulation domain: (a) a map of the Pampanga River basin and the locations of rain gauges, the Pantabangan dam, and the discharge gauging points, and b) a WRF-downscaling domain and topographical map at the 5-km spatial resolution.

The Pampanga River basin (Fig. 2a) is located in Central Luzon of the Philippines and the basin covers an area of 10,434 km^2. The basin receives an average annual rainfall of 2,155 mm. Due to its rich soil and water, the basin is a vital agricultural hub in the country and plays a crucial role in regional and national food security. However, the basin frequently faces threats from water-related disasters due to climate change. On average, the basin experiences at least one flood event per year, causing severe damage to agriculture, housing and infrastructure (Shrestha et al., 2016). For this study, hourly rainfall data were collected from 17 stations inside and outside the basin from 2009 to 2023 from the Philippine Atmospheric, Geophysical and Astronomical Services Administration (PAGASA). Figure 2a shows the locations of the daily rain gauges and their spatial distribution. To calibrate and validate the model of simulated streamflow, this research used discharge data collected at the San Isidro station during 2022–2023 (Fig. 2a).

The topographic data for the basin (i.e. digital elevation models, flow directions and flow accumulation) were obtained from the U.S. Geological Survey's (USGS) Hydrological Data and Maps Based on Shuttle Elevation Derivatives at Multiple Scales (HydroSHEDS). Figure 2 shows the spatial distribution of the DEM data used in the WEB-RRI modelling. The reclassified land-use data for the SiB2 model were obtained from USGS global datasets. Soil-type distribution data and related soil-water parameters, including three-layer saturated hydraulic conductivity values (i.e. surface soil, root zone and groundwater zone), soil porosity, residual soil moisture content and Van Genuchten parameters, were obtained from the Food and Agriculture Organization (FAO). The leaf area index (LAI) and the fraction of photosynthetically active radiation (FPAR) for incorporating vegetation phenology in the estimation of surface energy, water and carbon budget processes were obtained from the Moderate Resolution Imaging Spectroradiometer (MODIS) global products (MOD15A2) on the Terra satellite. Paddy area data for simulating the SIMRIW model were obtained from the Global Land Cover by National Mapping Organizations (GLCNMO). In addition to rainfall, meteorological forcing inputs such as air temperature, shortwave and longwave radiation, specific humidity, wind speed and surface pressure were obtained from the 55-year Japanese Reanalysis (JRA-55) products prepared by the Japan Meteorological Agency (JMA). This is one of the highest-quality, most homogeneous climate datasets covering the entire globe for the last half-century (Kobayashi et al., 2015). All of these gridded data were interpolated to model grid resolutions of ~450 m and temporal resolutions of ~1 hour.

2.3 Model setup

This study used climate outputs from the MRI-AGCM3.2H model (~60 km) and scaled these down to a 5 km grid using the Weather Research and Forecasting (WRF) model. The WRF model domain comprised 100 × 100 horizontal grids and 40 vertical layers (see Fig. 2b). It was calibrated using the WRF single-moment 3-class cloud microphysics scheme, the Mellor-Yamada-Nakanishi-Niino (MYNN) surface layer scheme, the unified Noah land-surface model and the MYNN level 2.5 boundary layer scheme. The study adopted the combined scaling and quantile mapping method proposed by Inomata et al. (2009) to correct the bias in the WRF-downscaled rainfall outputs.

The WEB-RRI model was adopted to simulate the basin's hydrological responses. It takes into account the dominant hydrological processes of a catchment area in a fully distributed manner (Rasmy et al., 2019), incorporating water and energy budget processes, land-vegetation-atmosphere interactions, multi-layer soil moisture dynamics and two-dimensional lateral water flow. This improves the simulation of processes such as interception, evaporation and transpiration, infiltration, groundwater flow, surface runoff and inundation. Due to its implicit treatment of basin-scale processes, the model is well-suited to long-term climate change simulations, enabling more accurate reproduction of hydrological responses to past climates, future projections and hydrological extremes.

This study also adopted the SIMRIW-Rainfed model, taking into account N-uptake and water stress (Homma and Horie, 2009). Additionally, the research implemented a formulation to consider the impact of flood depth and duration on rice damage and yield estimation. Although many factors change from the present to the future and affect rice production, this study only considered changes in meteorological factors such as rainfall, temperature, radiation and soil moisture. No changes were assumed in CO_2 concentration, fertiliser, irrigation and rice cultivars in the past or future. Only single cropping in the rainy season under rainfed conditions (no irrigation) was considered. The hybrid model exchanges radiation, temperature, root-zone soil moisture and inundation water depth, as calculated by the WEB-RRI model, for the SIMRIW-rainfed model at each identified paddy grid to simulate water stress, plant growth, damage due to water stress and flooding, and net yield. Conversely, the leaf area index (LAI) simulated by the SIMRIW-rainfed model is passed to the WEB-RRI model to simulate evapotranspiration processes and changes in soil moisture at each paddy grid.

2.4 3.3 Model performance evaluation indices

The Mean Bias Error (MBE), the Root Mean Square Error (RMSE), and the Nash-Sutcliffe Efficiency Coefficient (Nash), and spread (i.e. unbiased estimator of the standard deviation) were used for evaluating model performance on deterministic and ensemble mean estimation.

MBE is defined as:

$$MBE = \frac{\Sigma(O_i - \bar{O})}{N} \quad (1)$$

RMSE is defined as:

$$RMSE = \sqrt{\frac{\Sigma(O_i - S_i)^2}{N}} \quad (2)$$

Nash is defined as:

$$Nash = \frac{\Sigma(O_i - \bar{O})^2 - \Sigma(O_i - S_i)^2}{\Sigma(O_i - \bar{O})^2} \quad (3)$$

where O_i is the observation at i^{th} time, $\bar{O}$ is the average observation, S_i is the simulated value at i^{th} time, and N is the number of data.

3 RESULTS AND DISCUSSIONS

3.1 Future changes in temperature and rainfall

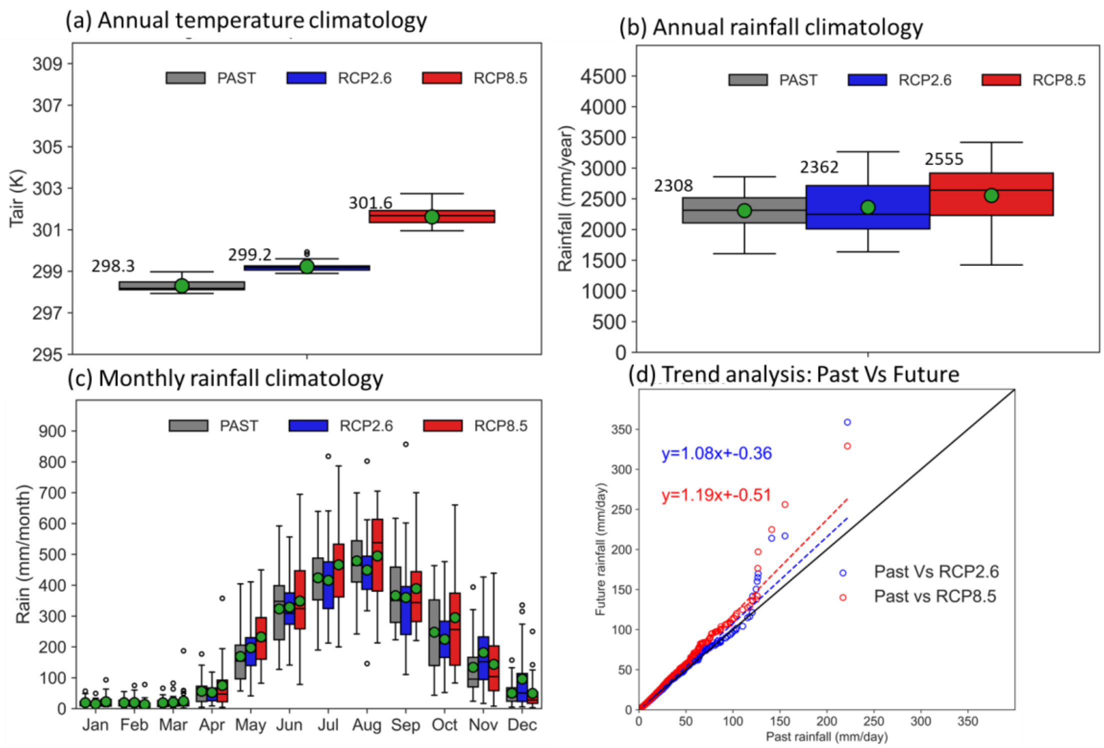

Figure 3: Comparison of basin-averaged climatology and extremes between historical and RCP scenario; (a) annual temperature climatology, b) annual rainfall climatology, c) monthly rainfall climatology, and c) rainfall trend analysis. The green circle in the box-whisker plot represents the mean values.

Figure 3a shows the comparison of the basin-averaged annual 2-meter air temperature climatology between the historical climate and the future climate projections under the RCP 2.6 and RCP 8.5 scenarios. The results show that the future climate will be warmer than the past climate. In particular, the warming is substantially greater under the RCP8.5 scenario (~3.3 K) than under the RCP2.6 scenario (~1 K) across the basin.

Figure 3b shows a comparison of the annual rainfall amounts in the past and future. The mean annual precipitation increases from approximately 2,308 mm/year in the historical period to approximately 2,362 mm/year under the RCP2.6 scenario (a 2.5% increase) and to approximately 2,555 mm/year under the RCP8.5 scenario (a 10.7% increase). In addition to the increase in mean rainfall, the RCP8.5 scenario exhibits greater variability, suggesting a higher likelihood of wet and dry years. The monthly rainfall climatology (Fig. 3c) shows that dry-season rainfall remains relatively low across all scenarios. In contrast, wet-season rainfall exhibits notable variations in median rainfall and increased variability in the future. Specifically, mean rainfall increases from April to June, indicating a stronger monsoon onset over the basin. Additionally, mean rainfall will decrease from July to October under the RCP2.6 scenario, while the RCP8.5 scenario shows increased mean rainfall during that period. Moreover, daily rainfall trend analysis shows that the intensity of rainfall (mm/day) will increase relative to the past. The regression slopes are 1.08 for RCP2.6 and 1.19 for RCP8.5, both of which exceed unity. Notably, the number of events with an intensity greater than 100 mm/day will be significantly higher under RCP8.5 than under RCP2.6, indicating more frequent and intense flooding events under RCP8.5.

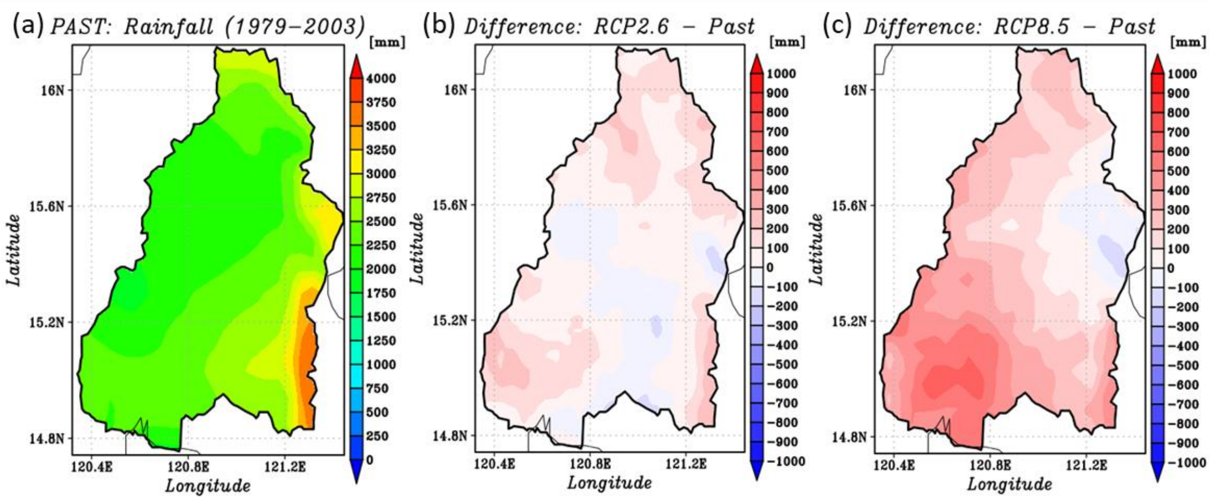

Figure 4: Comparison of spatial distribution of past and future annual rainfall climatology; a) past climate, b) changes in RCP2.6 scenario compared to past climatology, and c) changes in RCP8.5 scenario compared to past climatology

Figure 4a shows the spatial distribution of mean annual rainfall over the past period. It exhibits spatial variability, with localized zones of higher rainfall amounts along the eastern and southeastern parts of the basin. Figures 4b and 4c show the projected changes under the RCP2.6 and RCP8.5 scenarios, respectively, relative to past climate. The results suggest that under the RCP2.6 scenario, future rainfall will marginally change in the middle of the basin and moderately increase (by ~100–300 mm/year) in the rest of the region. Conversely, under RCP8.5, annual rainfall will increase more widely and significantly (~300–600 mm/year), particularly over the central and southern portions of the basin. Additionally, it should be noted that rainfall will decrease in the eastern part of the basin by ~100–200 mm/year, indicating the importance of developing sub-catchment-based water resource management policies for sustainable development.

3.2 WEB-RRI and SIMRIW model development, calibration, and validation

We developed the WEB-RRI-SIMRIW coupled model to assess the impact of meteorological changes under past and future Representative Concentration Pathway (RCP) climates on the basin's hydrological responses and rice yield. Based on our investigation, reliable discharge data from 2022 to 2023 was used for calibration and validation. Additionally, rain-fed crop yield data from the Pampanga province was limited and only available from 2017 to 2019. We simulated the WEB-RRI and SIMRIW models from 2017 to 2023, using Pantabangan dam outflow records as boundary conditions.

Figure 5(a) compares observed and WEB-RRI model-simulated discharges from January 1 to December 31, 2002. This period includes the recorded flood event and was used for model calibration. As shown in the figure, the WEB-RRI model was reasonably well calibrated (Nash = 0.6, RMSE = 84 m^3/s). Though the model captured the peak flow during the typhoon period well, it underestimated it. This could be due to uncertainties in heavy rainfall observations and measurement techniques. Furthermore, Fig. 7(b) shows that the model simulated river low and peak discharges during the validation period that matched the observed discharges well (Nash = 0.68, RMSE = 82 m^3/s).

Figure 6 compares recorded and simulated rice yield data under non-irrigated conditions in the Pampanga province from 2015 to 2019. Observed yields remained relatively stable at approximately 410–430 g/m^2, and the SIMRIW simulations captured the yield estimation relatively well, comparable to the observations (MBE = -9.6 g/m^2 and RMSE = 41.5 g/m^2). Though the observed records are limited to five years, these simulations provide valuable insights into the mean and variability of yields, highlighting the potential of the SIMRIW rain-fed model for assessing rice productivity in the context of climate change.

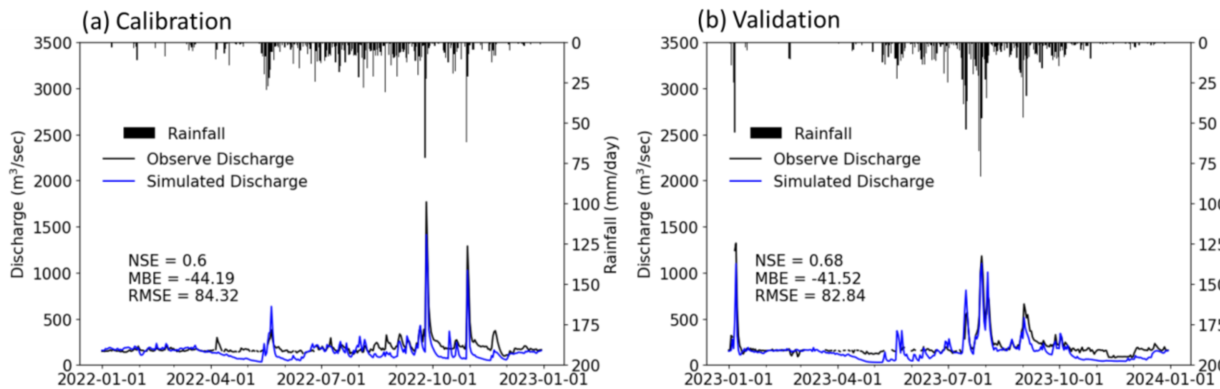

Figure 5: Comparison between observed discharge and simulated discharge at the SanIsidro gauging station: (a) model calibration for 2002 and (b) model validation for 2023

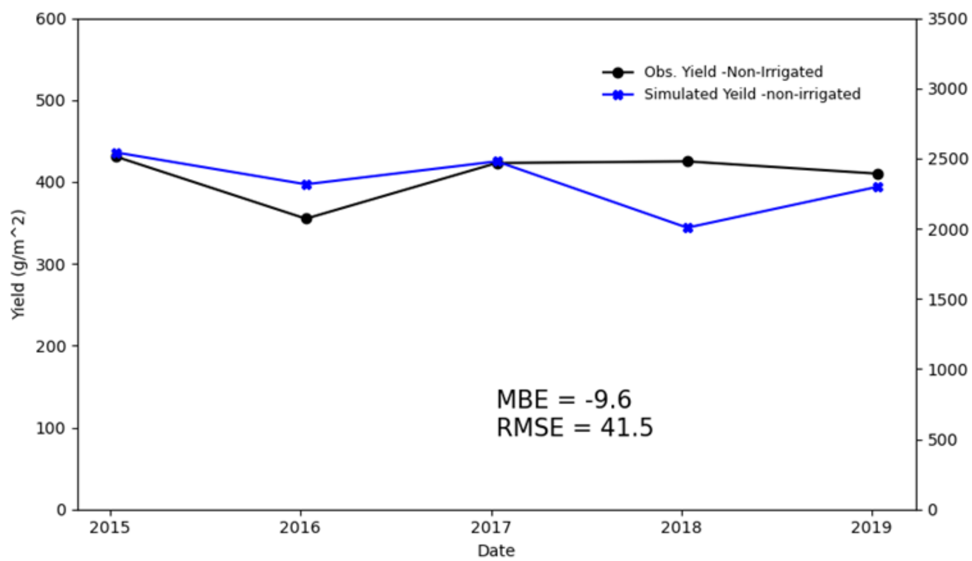

Figure 6: Comparison between reported and simulated yields of non-irrigated paddy from 2015 to 2019

3.3 Future changes in hydrological parameters

Figure 7(a) compares the annual climatology of river discharge at the San Isidro gauging station for past climates and future projections under the RCP 2.6 and RCP 8.5 scenarios. The results indicate a marginal (~1%) increase in mean discharge under RCP2.6 and a moderate (~5%) increase under RCP8.5. More importantly, the RCP8.5 scenarios exhibit greater variability and a higher probability of extreme high and low flow conditions. At the same time, the mean monthly climatology of river discharge (Fig. 7b) increases at the onset of the wet season (i.e., May–July), with the strongest amplification observed under RCP8.5. This implies an elevated risk of seasonal flooding and crop cultivation damage, as this period coincides with sowing and the early stages of crop growth. Additionally, it can be noted that the monthly mean and median discharges decrease under both future projections during August–October, highlighting the trend of water scarcity for food production. Trend analysis of daily discharges (Fig. 7c) reveals that hydrological events with a flow rate greater than 1,000 m^3/s will be more frequent under

RCP8.5. However, flow rates greater than 2,000 m³/s will be more frequent under RCP2.6 than in the past. Therefore, these results further highlight the amplification of extremes in the future climate under both projections. Specifically, there will be more flood events, and low-flow events (<50 m³/s) will be more frequent (Fig. 7d) under RCP8.5.

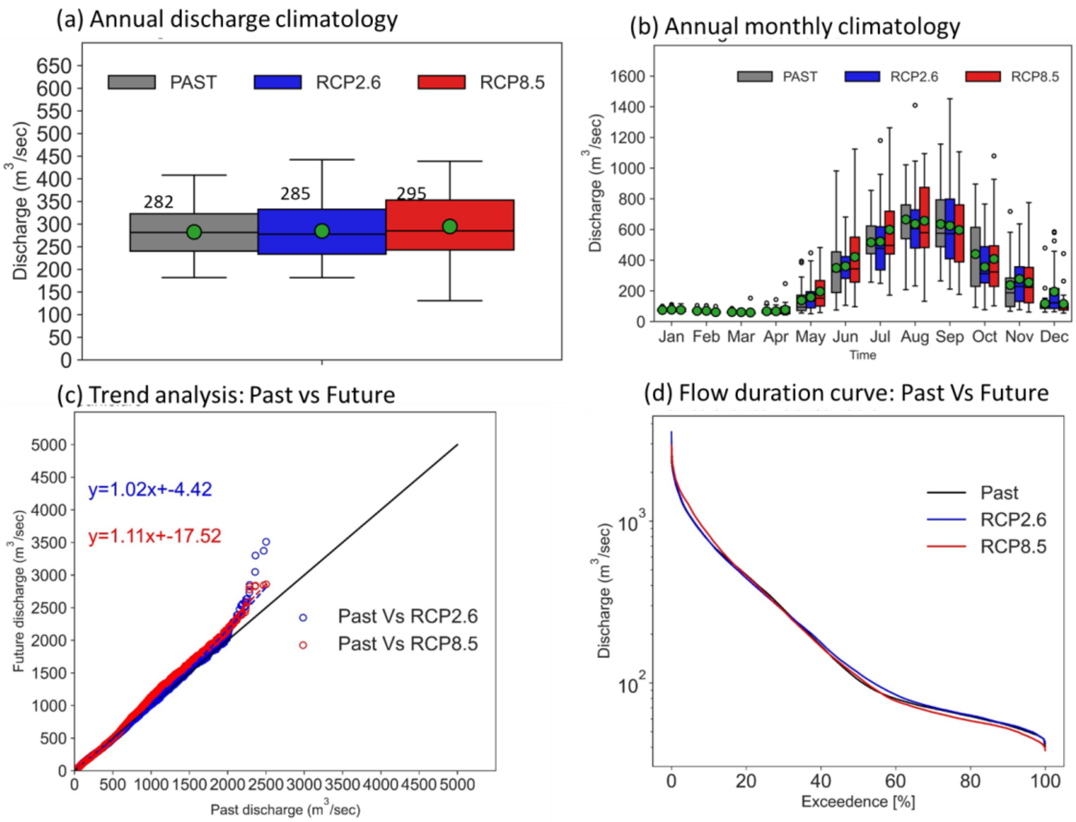

Figure 7: Comparison of basin-averaged discharge climatology and extremes at San-Isidro gauging station between historical and RCP scenario; (a) annual discharge climatology, b) annual monthly climatology, c) trend analysis of daily discharges, and d) flow duration curve. The green circle in the box-whisker plot represents the mean values.

3.4 Future changes in paddy yield

We used the calibrated WEB-RRI-SIMRIW model to simulate crop yields at the basin scale, and investigated the model outputs to assess the simultaneous impact of temperature increases, water stress, and flood inundation on paddy yields. Figure 8(a) shows the spatial distribution of rice yields across the basin under past climate conditions. As the figure shows, the simulation results indicate an average yield of around 500 g/m² in the basin and around 350 g/m² in the frequently flooding Candaba region. Figure 8(b) presents the projected mean change in yield under RCP2.6 relative to past climate conditions. Most of the basin exhibits marginal yield reductions (20 to 100 g/m²), while localized yield gains (50 to 100 g/m²) are evident in the Candaba area. Conversely, Fig. 8c shows that the projected mean yield change under RCP8.5 is more widespread and severe. Extensive areas show losses of up to 50-150 g/m².

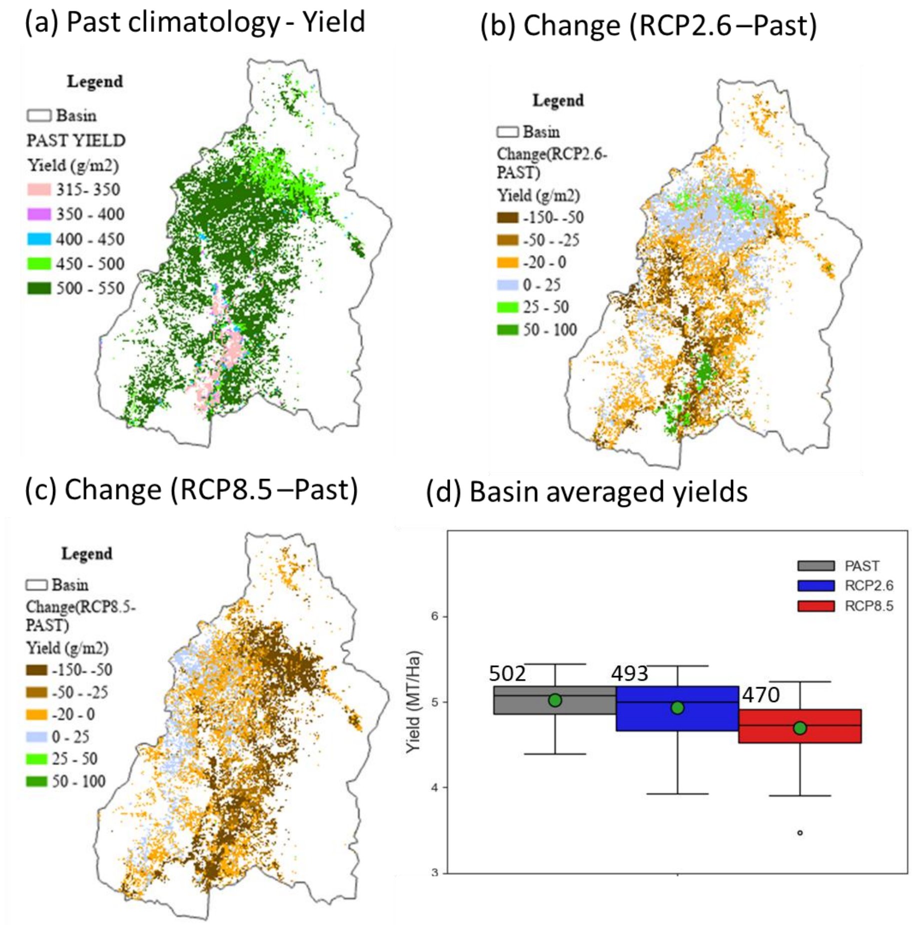

Figure 8: Comparison in annual average rain-fed -paddy yield between historical and RCP8.5 scenario; a) past climatology (g/m^2), b) changes in RCP2.6 projection compared to past (g/m^2), and c) changes in RCP8.5 projection compared to past (g/m^2), and d) basin averaged yield (MT/Ha)

The box plots (Fig. 8d) summarize basin-wide yield statistics for the historical period and future projections. The mean yield is expected to decrease by ~1.6% under RCP2.6 and by an additional 6.3% under RCP8.5 compared to past climate yields. Notably, the variability of yields under future RCPs shifts toward lower values, not only the mean values. The future climate under RCP8.5 shows that intensified climate change leads to reduced average productivity and greater uncertainty. This intensified climate change includes warming, increased flood intensity and frequency, and decreased low flow rates. Overall, these results demonstrate that average yields will not only reduce under emission scenarios but also exhibit greater risk and uncertainty, which are critical concerns for agricultural resilience and food security in the basin.

4 CONCLUSIONS

Reliably assessing the impacts of climate change on the water-food nexus is crucial for developing policies that build climate-resilient and sustainable societies. This study provides a thorough evaluation of climate change's effects on rainfall, river discharge, and water yield at the basin level, considering two different climate projections (RCP2.6 and RCP8.5), in the Pampanga basin. Projected results for the future climate show an intensification of the hydrological cycle with increased annual rainfall, an intensified monsoon onset, and amplified extreme rainfall events and intensity. We translated these meteorological changes using a seamless Water and Energy Budget-based Rainfall-Runoff-Inundation (WEB-RRI) model coupled with the Simulation Model for Rice-Weather Relations (SIMRIW) model. This allowed us to produce a basin response with respect to water availability, hydrological extremes, and food production. The results indicate that annual river discharge at the San-Isidro gauging station will increase, especially during monsoon onset, and that the frequency and intensity of extreme high-discharge events will increase, which highlights the amplified flood risk under future climate conditions. Crop yield projections show a predominantly negative response to climate change. Moderate emissions (i.e., RCP2.6) result in relatively minor yield reductions, while high emissions (i.e., RCP8.5) lead to significant and widespread yield losses across the basin. The combined effects of climate change, including rising temperatures, altered rainfall seasonality, and increased hydrological extremes, will likely exacerbate stress on water and food security and threaten the long-term sustainability of the basin. The findings of this study provide valuable scientific evidence to support climate-informed planning, disaster risk reduction, and adaptive water and agriculture policies in the basin.

5 ACKNOWLEDGEMENTS

This research was supported by the Science and Technology Research Partnership for Sustainable Development (SATREPS) program, which is implemented in collaboration with Japan and the Philippines. The authors would like to thank the University of Tokyo for providing resources for data archiving, processing, model simulations, and evaluation through the Data Integration and Analysis System (DIAS), as well as PAGASA for providing the necessary data for developing and validating the hydrological model.

REFERENCES

IPCC, 2022: Climate Change 2022: Impacts, Adaptation, and Vulnerability. Contribution of Working Group II to the Sixth Assessment Report of the Intergovernmental Panel on Climate Change [H.-O. Pörtner, D.C. Roberts, M. Tignor, E.S. Poloczanska, K. Mintenbeck, A. Alegría, M. Craig, S. Langsdorf, S. Löschke, V. Möller, A. Okem, B. Rama (eds.)]. Cambridge University Press. Cambridge University Press, Cambridge, UK and New York, NY, USA, 3056 pp., doi:10.1017/9781009325844

Kusunoki, S. and O. Arakawa, 2015: Are CMIP5 models better than CMIP3 models in simulating rainfall over East Asia? J. Clim. 28, 5601–5621

Rockel, B., 2015: The regional downscaling approach: A brief history and recent advances, Curr. Clim. Change Rep., 1(1), 22–29

Moghim, S., Bras, R.L., 2017: Bias Correction of Climate Modeled Temperature and Precipitation Using Artificial Neural Networks. J. Hydrometeorology, 18, 1867–1884.

Sayama, T, G. Ozawa, T. Kawakami, S. Nabesaka, and K. Fukami, 2012: Rainfall-Runoff-Inundation Analysis of Pakistan Flood 2010 at the Kabul River Basin, Hydrological Sciences Journal, 57(2), pp. 298-312.

Zheng, Y., J. Li, T. Zhang, Y. Rong, and P. Feng, 2021: Exploring the Application of Flood Scaling Property in Hydrological Model Calibration, Journal of Hydrometeorology, 22(12), 3255-3274

Rasmy, M., T. Sayama, T. Koike, 2019: Development of water and energy Budget-based Rainfall-Runoff -Inundation model (WEB-RRI) and its verification in the Kalu and Mundeni River Basins, Sri Lanka. J. Hydrol. 579, 124163

Horie, T., Nakagawa, H., Centeno, H., Kropff, M., 1995: The rice crop simulation model SIMRIW and its testing. In: Matthews, R.B., Kropff, M.J., Bachelet, D., van Laar, H.H.

(Eds.), Modeling the Impact of Climate Change On Rice Production. CAB International, AsiaOxon, U.K., pp. 51–66.

Homma, K., Maki, M., Hirooka, Y., 2017: Development of a rice simulation model for remote-sensing (SIMRIW-RS). J. Agric. Meteorol. 73, 9–15. https://doi.org/10.2480/agrmet.d-14-00022.

Maki, M., Sekiguchi, K., Homma, K., Hirooka, Y., Oki, K., 2017. Estimation of rice yield by SIMRIW-RS, a model that integrates remote sensing data into a crop growth model. J. Agric. Meteorol. 73, 2–8. https://doi.org/10.2480/agrmet.D-14-00023.

Raksapatcharawong, M., Veerakachen, W., Homma, K., Maki, M., & Oki, K., 2020: Satellite-Based Drought Impact Assessment on Rice Yield in Thailand with SIMRIW-RS. Remote Sensing, 12(13), 2099. https://doi.org/10.3390/rs12132099

Inomata, H., K. Takeuchi, K. Fukami, 2009: Development of a statistical bias correction method for daily rainfall data of GCM20. Annu J Hydraul Eng 55, 247–252